EXTENDED PDF FORMAT
SPONSORED BY

BIO-RAD

http://discover.bio-rad.com



Abiotic Forcing of Plankton Evolution in the Cenozoic

Daniela N. Schmidt, *et al.*

Science **303**, 207 (2004);
DOI: 10.1126/science.1090592

The following resources related to this article are available online at www.sciencemag.org (this information is current as of January 2, 2007):

Updated information and services, including high-resolution figures, can be found in the online version of this article at:
http://www.sciencemag.org/cgi/content/full/303/5655/207

Supporting Online Material can be found at:
http://www.sciencemag.org/cgi/content/full/303/5655/207/DC1

This article **cites 12 articles**, 10 of which can be accessed for free:
http://www.sciencemag.org/cgi/content/full/303/5655/207#otherarticles

This article has been **cited by** 10 article(s) on the ISI Web of Science.

This article has been **cited by** 2 articles hosted by HighWire Press; see:
http://www.sciencemag.org/cgi/content/full/303/5655/207#otherarticles

This article appears in the following **subject collections**:
Oceanography
http://www.sciencemag.org/cgi/collection/oceans

Information about obtaining **reprints** of this article or about obtaining **permission to reproduce this article** in whole or in part can be found at:
http://www.sciencemag.org/help/about/permissions.dtl

Downloaded from www.sciencemag.org on January 2, 2007

Science (print ISSN 0036-8075; online ISSN 1095-9203) is published weekly, except the last week in December, by the American Association for the Advancement of Science, 1200 New York Avenue NW, Washington, DC 20005. Copyright c 2006 by the American Association for the Advancement of Science; all rights reserved. The title SCIENCE is a registered trademark of AAAS.

28. P. E. Damon, R. E. Sternberg, *Radiocarbon* **31**, 697 (1989).
29. The same experiment was performed with the use of a zonally averaged global ocean circulation model with atmospheric and biospheric carbon exchange as described in (*38*). The more detailed model produced atmospheric $\Delta^{14}C$ for the past 50 ka B.P. within ±10‰ of the simple box model. Subsequent glacial perturbation experiments were carried out in the box model as a computational expedient.
30. Measurements of air bubbles in ice cores show that glacial atmospheric CO_2 concentration averaged ~200 parts per million by volume (ppmv) compared to a preindustrial value of ~280 ppmv (*39*). A reduction of terrestrial biomass to 65% of its preindustrial size is within the bounds of previous estimates (*40*) and is necessary to balance a lowering of glacial $\delta^{13}C$ of oceanic ΣCO_2 by an average of −0.3‰ (*41*).
31. Reduced deep-ocean ventilation is consistent with potentially restricted NADW formation and penetration in the glacial ocean. Global transects of radiocarbon distribution in the oceans suggest that NADW formation is responsible for sequestering up to 75% of the radiocarbon in the deep ocean (*42*).
32. This change represents a 120-m lowering of sea level and the resultant shift of carbonate sedimentation off the continental shelves into deep water, where dissolution is much more extensive. Discussion and details of the glacial carbon cycle boundary conditions are summarized in SOM Text, fig. S3, and table S2.
33. L. D. Keigwin, S. J. Lehman, *Paleoceanography* **9**, 185 (1994).
34. J. F. McManus, R. Francois, J.-M. Gherardi, L. D. Keigwin, S. Brown-Leger, in preparation.
35. W. B. Curry, T. M. Marchitto, J. F. McManus, D. W. Oppo, K. L. Laarkamp, in *Mechanisms of Global Climate Change at Millennial Time Scales*, P. U. Clark, R. S. Webb, L. D. Keigwin, Eds. (American Geophysical Union, Washington, DC, 1999), vol. 112, p. 59.
36. T. F. Stocker, D. G. Wright, *Radiocarbon* **40**, 359 (1998).
37. M. Stuiver, H. A. Polach, *Radiocarbon* **19**, 355 (1977).
38. O. Marchal, T. F. Stocker, R. Muscheler, *Earth Planet. Sci. Lett.* **185**, 383 (2001).
39. A. Indermuhle, E. Monnin, B. Stauffer, T. F. Stocker, M. Wahlen, *Geophys. Res. Lett.* **27**, 735 (2000).
40. K. D. Alverson, R. S. Bradley, T. F. Pederson, Eds., *Paleoclimate, Global Change and the Future* (Springer Verlag, New York, 2003).
41. W. B. Curry, J.-C. Duplessy, L. D. Labeyrie, N. J. Shackleton, *Paleoceanography* **3**, 317 (1988).
42. W. S. Broecker, *Science* **300**, 1519 (2003).
43. This work was supported by NSF (OCE-0117356), Lawrence Livermore National Laboratory (LDRD-97-ERI-009), and the U.S. Department of Energy (W-7405-Eng-48). We thank the ODP Core Repository in Bremen for core sampling; B. Frantz and P. Zermeno for sample preparation assistance; C. Laj, M. Frank, J.-P. Valet, and J. Stoner for providing their data of past geomagentic field intensities; and S. Johnsen for making available the revised GRIPss09sea chronology. This is WHOI contribution no. 11061.

Supporting Online Material

www.sciencemag.org/cgi/content/full/303/5655/202/DC1
Materials and Methods
Figs. S1 to S4
Tables S1 and S2

11 August 2003; accepted 25 November 2003

Downloaded from www.sciencemag.org on January 2, 2007

REPORTS

Abiotic Forcing of Plankton Evolution in the Cenozoic

Daniela N. Schmidt,*† Hans R. Thierstein, Jörg Bollmann, Ralf Schiebel

We characterize the evolutionary radiation of planktic foraminifera by the test size distributions of entire assemblages in more than 500 Cenozoic marine sediment samples, including more than 1 million tests. Calibration of Holocene size patterns with environmental parameters and comparisons with Cenozoic paleoproxy data show a consistently positive correlation between test size and surface-water stratification intensity. We infer that the observed macroevolutionary increase in test size of planktic foraminifera through the Cenozoic was an adaptive response to intensifying surface-water stratification in low latitudes, which was driven by polar cooling.

A long-standing controversy surrounds the relative importance of biotic controls (such as competition, predation, grazing, and infection) versus abiotic forcing (such as climate, geography, bolide impacts, and volcanism) in shaping the evolution of life on Earth (*1*, *2*). A few exemplary morphometric studies of marine microfossils have focused on the ecological aspects of evolutionary change (*3*, *4*), although most have concentrated on the stratigraphic patterns of size and shape changes (*5*–*7*). Macroevolutionary processes—evolution above the species level—may be characterized by changes in diversity, longevity, speciation and extinction rates, and the size of fossil organisms (*8*). Body size, an easily measured indicator of macroevolution, is related to biological processes (*9*), notably metabolism, growth rate, and resistance to starvation and predation, and to environmental factors (*9*). However, little has been known about such relationships in the past. The dearth of data and consequently slow progress has mainly been due to the laboriousness of collecting morphometric measurements.

In order to avoid this difficulty, we have used automated microscopy (*10*) to measure the size distributions of entire planktic foraminiferal assemblages in 69 Holocene (*11*) and 454 Cenozoic (*12*) globally distributed deep-sea samples (for a total of 10^6 shells), from 18 high- and low-latitude Deep-Sea Drilling Program (DSDP) and Ocean Drilling Program (ODP) drill sites (table S1). All size spectra measured are from the >150-μm fractions and are strongly right-skewed. Means, maxima, and 95th percentiles are highly correlated with each other and generally increase with surface-water temperature (*11*). Following Chapelle and Peck (*13*), we used the 95th percentile, i.e., the size that separates the smaller 95% of individuals from the largest 5% (the $size_{95/5}$) (*11*, *14*). These size measurements allow us to address a very fundamental but still elusive question in paleobiology: Is the observed evolutionary size increase the result of a random increase in variance (*15*, *16*), or is it mainly due to biotic interactions (*1*) or to abiotic forcing (*2*)?

Since the early Cretaceous [~140 million years ago (Ma)], planktic foraminifera have undergone at least three episodes of major evolutionary radiation (*17*, *18*), each of which is thought to have involved increases in test size (*16*). These increases started at 132 Ma, 65 Ma, and 33 Ma (*16*). The main features of our data set on $size_{95/5}$ evolution of planktic foraminifera since the late Cretaceous are most apparent when grouped into low- and high-latitude averages for one-million-year (1-My) intervals (Fig. 1A). The major emerging characteristic is that $size_{95/5}$ development was coherent in both low- and high-latitude assemblages up to 42 Ma (mid-Eocene) and has diverged since. The sudden $size_{95/5}$ decrease at the Cretaceous/Paleogene boundary 65 Ma (*19*) was global and is linked to the impact-related mass extinction of most planktic foraminiferal species. In high-latitude records from the Kerguelen Plateau, Rockall Plateau, Walvis Ridge, and Rio Grande Rise, the $size_{95/5}$ of planktic foraminiferal assemblages remained dominantly small and never recovered to their late Cretaceous values (*12*). In low-latitude areas, the $size_{95/5}$ development can be divided into four time intervals based on the $size_{95/5}$ relationship to the Cenozoic mean ($size_{95/5}$ = 389 μm): an interval of dwarfed assemblages (65 to 59 Ma) until $size_{95/5}$ reached the Cenozoic average for the

Department of Earth Sciences, Eidgenössische Technische Hochschule (ETH) Zürich, and University of Zürich, ETH-Zentrum, CH-8092 Zürich, Switzerland.

*Present address: Department of Geology, Royal Holloway, University of London, Egham, Surrey TW20 OEX, UK.
†To whom correspondence should be addressed. E-mail: d.schmidt@gl.rhul.ac.uk

first time, followed by a prolonged interval of small $size_{95/5}$ below the Cenozoic mean (59 to 42 Ma), then by a transitional interval (42 to 12 Ma) with $size_{95/5}$ variation around the Cenozoic mean, and finally by a marked and unprecedented $size_{95/5}$ increase in the late Neogene (Fig. 1A). From the end of the Miocene onward, low-latitude planktic foraminiferal $size_{95/5}$ have been consistently larger than they had ever been before.

To test for possible links between the $size_{95/5}$ development of planktic foraminifera and environmental change, we first compared the $size_{95/5}$ of Holocene assemblages with various environmental parameters (*11*). Among these, the temperature and thermal structure of the upper water column (0 to 200 m) showed the highest correlations with $size_{95/5}$. The general $size_{95/5}$ increase with increasing sea surface temperature is interrupted by smaller $size_{95/5}$ in frontal areas, such as the polar fronts at ~2°C and the subtropical fronts around 18°C (Fig. 2A). Our data (*11*) confirm earlier observations (*20*) that single planktic foraminiferal species are most abundant and grow to their largest sizes at specific temperatures (*20*). Such optimum conditions seem to be located in the hydrographically more stable areas and are absent (*11*, *20*) at the temperatures characteristic of the frontal areas (Fig. 2B). We have also explored the correlation of foraminiferal $size_{95/5}$ with surface water stratification, expressed as the temperature difference between the surface and 200-m water depth (Fig. 2C). This stratification index shows a significantly higher correlation with $size_{95/5}$ (Pearson's product moment correlation $r^2 = 0.547$, $P < 0.001$) than with species richness (*11*) ($r^2 = 0.284$, $P < 0.001$). Using an independent data set (*21*), we can show that the temperature gradient in the top 200 m of the water column is also reflected in the observed maximum oxygen stable isotope ration ($\delta^{18}O$) differences between shallow- and deep-dwelling Holocene planktic foraminiferal species (Fig. 2D). This latter stratification indicator will be crucial in the following interpretation of the Cenozoic size record.

In our search for potential forcing mechanisms, we compared the observed $size_{95/5}$ changes in Cenozoic planktic foraminifera with available records of paleoenvironmental proxies, such as various isotopic and elemental ratios (*12*). These are thought to describe past changes in climate, ocean circulation, and global carbon chemistry (*22*). Our Cenozoic $size_{95/5}$ record shows a crude similarity with the oxygen isotope record based on benthic foraminifera (*23*), which primarily reflects changes in high-latitude temperatures and ice volume (Fig. 1, A and B). Less positive $\delta^{18}O_{benthic}$ values are associated with small $size_{95/5}$ ($r^2 = 0.719$, $P < 0.001$) and the pronounced gradual $size_{95/5}$ increase in the late Neogene parallels an equally gradual increase in average $\delta^{18}O_{benthic}$ values. This appears to support Lipps' hypothesis of a causal relationship between the iterative evolution of planktic foraminiferal diversity and the changing vertical and particularly horizontal temperature gradients proposed long ago (*24*).

High-latitude and deep-water cooling would necessarily lead to a steepening of the thermocline in low-latitude areas. The most appropriate test would therefore be a comparison between the observed $size_{95/5}$ changes in low-latitude planktic foraminiferal assemblages and the available evidence for vertical and latitudinal temperature gradients as expressed in the oxygen isotopic differences between various shallow- and deep-dwelling planktic foraminiferal species. To this end, and to eliminate ice effects, we have

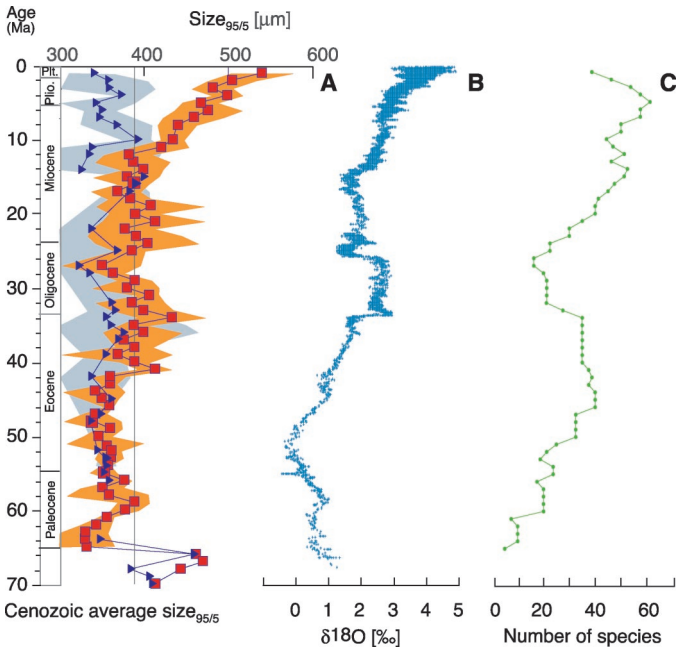


Fig. 1. Cenozoic changes in test $size_{95/5}$ of planktic foraminiferal assemblages in low and high latitudes, in high-latitude cooling represented by $\delta^{18}O$ ratios of benthic foraminifera, and in global species richness. Test sizes are given as test $size_{95/5}$ (*13*), which is the size separating the largest 5% of an assemblage from the rest. (**A**) 1-My means for planktic foraminiferal assemblage $sizes_{95/5}$ from tropical and subtropical sites (squares) and from temperate and subpolar sites (triangles). The vertical line shows the mean $size_{95/5}$ (389 µm) of all assemblages. Light blue and orange shading shows ±1 standard deviations for mean $sizes_{95/5}$. Plio., Pliocene; Plt., Pleistocene. (**B**) The global deep-sea oxygen isotope record representing Cenozoic polar cooling and ice accumulation (*23*). (**C**) The total number of planktic foraminiferal species globally known per 1-My interval (*18*).

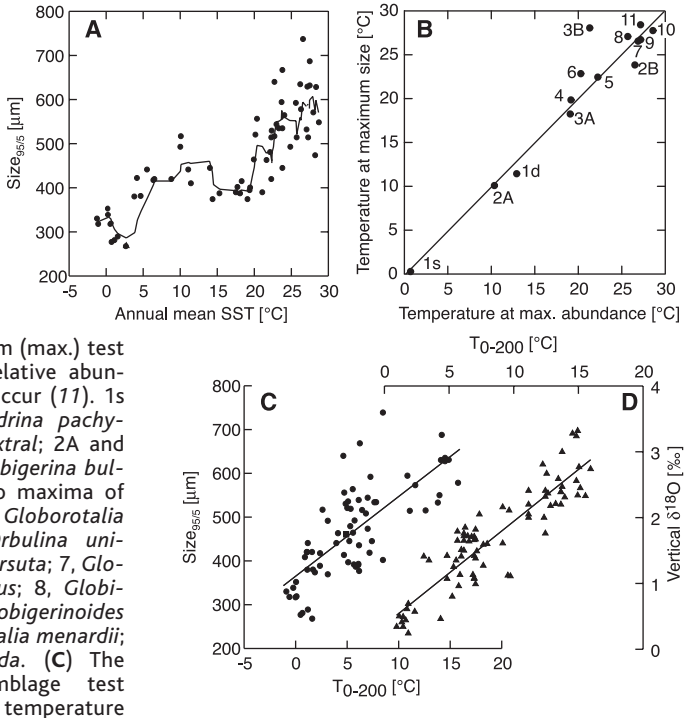


Fig. 2. Test size variability of planktic foraminifera in Holocene samples. (**A**) $Size_{95/5}$ versus annual mean sea-surface temperatures (SST) in 69 Holocene samples. The line shows the 5-point moving average. (**B**) The correlation ($r^2 = 0.928$, $P < 0.001$) of surface-water temperatures at which maximum (max.) test sizes and maximum relative abundances of single taxa occur (*11*). 1s and 1d, *Neogloboquadrina pachyderma sinistral* and *dextral*; 2A and 2B, two maxima of *Globigerina bulloides*; 3A and 3B, two maxima of *Globorotalia inflata*; 4, *Globorotalia truncatulinoides*; 5, *Orbulina universa*; 6, *Globorotalia hirsuta*; 7, *Globigerinoides conglobatus*; 8, *Globigerinoides ruber*; 9, *Globigerinoides sacculifer*; 10, *Globorotalia menardii*; 11, *Globorotalia tumida*. (**C**) The correlation of assemblage test $size_{95/5}$ with vertical temperature difference (T_{0-200}) in the top 200 m (circles) (*11*). (**D**) The correlation of T_{0-200} and maximum difference in oxygen isotopic ratios among shallow- and deep-dwelling Holocene planktic foraminifera in 108 south Atlantic samples (triangles) (*21*) (table S4). Lines in (C) and (D) represent linear correlations.

Downloaded from www.sciencemag.org on January 2, 2007

compiled published isotope measurements of various planktic species in single samples from the sites used in our study (table S2). Because multispecies isotope analyses are not very abundant and to emphasize long-term trends over regional and short-term variability, we have extracted the largest oxygen isotope difference among planktic species within single samples and the largest oxygen isotope range between low- and high-latitude shallow-dwelling species throughout the Cenozoic. To avoid the potential bias of diminishing availability, with increasing age, of samples with multispecies isotope analyses, we sorted the samples by their age and extracted the largest isotope gradients from eight groups of seven samples each (table S3). Using the maximum gradients instead of an average minimizes the potential influence of diagenesis, which would decrease the range of values observed in a single sample (*25*). The high correlation of maximum and average values per group ($r^2 = 0.972$ $P, < 0.001$) shows that the maxima used here are not odd outliers.

When we compared the oxygen isotope gradients with the $size_{95/5}$, marked trends and correlations resulted (Fig. 3). Both the maximum latitudinal $\delta^{18}O$ range and the maximum latitudinal $size_{95/5}$ range evolved ($r^2 = 0.881$, $P < 0.001$) during the Cenozoic along a tightly constrained trajectory (Fig. 3A). A comparably high correlation ($r^2 = 0.951$, $P < 0.001$) along a similar trajectory is observed between the computed maximum vertical $\delta^{18}O$ differences among planktic foraminiferal species and the maximum $size_{95/5}$ (Fig. 3B).

These strong positive correlations between $size_{95/5}$ and the proxies for latitudinal and vertical temperature gradients in surface waters call for an ecological interpretation. Whereas our compilations average out a considerable amount of smaller scale variability related to local conditions, the evidence indicates that increasing global latitudinal and vertical temperature gradients have promoted growth of planktic foraminifera to larger sizes. Polar cooling induced greater latitudinal temperature ranges and stronger temperature stratification of low-latitude surface waters and thus a larger number of available ecological niches (*26*, *27*). Why this may have led to larger test sizes must currently remain speculative, because too little is known about the processes that control differential test size development in living planktic foraminifera. Nevertheless, increase in size and weight may be a consequence of delayed reproduction under unfavorable conditions, or it may have allowed planktic foraminifera to migrate to greater depth during their life cycle (*26*). In addition, the test size increase may have improved fitness through an increased number of symbionts, better resistance to predation, a higher gamete yield, an enhanced differential floating ability that allows species-specific gamete release at distinct density surfaces, or better food exploitation near an evolving deep chlorophyll maximum.

We accepted the foregoing interpretation only after we had carefully considered and then rejected the following alternative interpretations for the data at hand. Body size increase could have been a direct physiological response to temperature change. This seems unlikely, however, for two reasons. First, there is little evidence for a $size_{95/5}$ decrease in the cooling high latitudes; second, the most pronounced $size_{95/5}$ increase occurred in the low latitudes, where surface-water temperatures may not have changed much in the Cenozoic (*25*). Carbonate saturation changes are probably not causative either, because the reconstructed history of seasurface alkalinity changes shows its highest values in the Paleogene (*28*), whereas the most marked $size_{95/5}$ increase for planktic foraminifera occurs in the late Neogene (*12*).

Size changes might also be directly correlated to species richness, which is the result of differential changes in speciation and extinction rates. Both of these were probably influenced by climate change (*27*). In addition, diverse assemblages are more likely to include a few species that grow to larger size than low-diversity assemblages, and thus some correlation of size and species richness data can be expected (Fig. 1C). However, the correlation coefficient between the available Cenozoic species richness (*18*) and $size_{95/5}$ is rather low ($r^2 = 0.388$, $P < 0.001$ for 1-My averages), indicating that diversity is not the main driver of the observed $size_{95/5}$ changes (*12*).

The published stable-isotope gradients among different species of planktic foraminifera that we use might have been progressively influenced by diagenetic alteration with increasing age and burial depth (supporting online text). We consider the oxygen isotopic evidence for stratification changes as real for several reasons. The strongest of these is the indication that the comparatively large $size_{95/5}$ near the end of the Cretaceous (Fig. 1A) coincide with increased isotopic gradients. Multispecies isotope measurements from the end of the Cretaceous are rather rare and are totally absent from the sites in which we document the relatively large $size_{95/5}$ of Maastrichtian planktic foraminifera. However, maximum oxygen-isotope gradients within the best-preserved, latest-Cretaceous, planktic foraminiferal assemblages cover a range of up to 1.9 per mil (‰) in Tanzania (*25*), 1.7‰ at ODP Site 1050 (*29*), and 1.8‰ at DSDP Site 356 (table S5). Latitudinal surface-water gradients at the end of the Cretaceous also seem to have been higher than in the Paleogene, as evidenced by the 2.3‰ difference in *Heterohelix globulosa* from high and mid-latitudes (*30*).

We conclude that the evolutionary size development of planktic foraminifera in space and through time was made adaptively possible by changing global climates and that it is not just the result of accumulating variance, which might be linked to increasing species richness (*15*, *16*). Future studies combining multispecies oxygen isotopes with size measurements in identical samples will provide appropriate tests for our proposition. Abiotic forcing of the macroevolutionary size increase is coherent with predictions of the stationary model of evolution (*2*), and we find little support for the Red Queen model (*1*), which describes the dependence of evolutionary change on biotic controls.

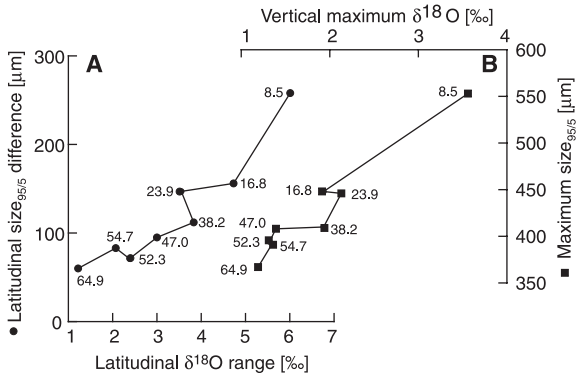


Fig. 3. Cenozoic coevolution of planktic foraminiferal test sizes and oxygen-isotope gradients in surface waters. All values were extracted from 164 published multispecies isotope analyses (tables S2 and S3), which were grouped into eight time intervals, each encompassing seven samples. The age (in Ma) of the beginning of the intervals is labeled along the macroevolutionary trajectories. (**A**) The correlated increase of maximum latitudinal $\delta^{18}O$ range of shallow-dwelling planktic foraminifera and of latitudinal $size_{95/5}$ range through the Cenozoic (circles). (**B**) The correlated increase of maximum vertical $\delta^{18}O$ difference among shallow- and deep-dwelling planktic foraminifera species in single assemblages and of maximum assemblage $size_{95/5}$ through the Cenozoic (squares). The shown increase in isotope gradient is equivalent to a 12°C increase in the water-temperature gradient between shallow- and deep-dwelling planktic foraminifera.

References and Notes

1. L. van Valen, *Evol. Theory* **1**, 1 (1973).
2. N. C. Stenseth, J. Maynard Smith, *Evolution* **38**, 870 (1984).
3. K. Kaiho, *Geology* **26**, 491 (1998).
4. R. D. Norris, R. M. Corfield, J. Cartlidge, *Paleobiology* **22**, 386 (1996).
5. A. Arnold, *Paleobiology* **9**, 390 (1983).
6. B. A. Malmgren, W. A. Berggren, G. P. Lohman, *Paleobiology* **9**, 377 (1983).
7. A. J. Arnold, D. C. Kelly, W. C. Parker, *J. Paleontol.* **69**, 203 (1995).
8. S. M. Stanley, *Macroevolution Pattern and Process* (John Hopkins Univ. Press, Baltimore, 1998).
9. R. H. Peters, *The Ecological Implications of Body Size* (Cambridge Univ. Press, Cambridge, 1983).
10. J. Bollmann *et al.*, in *Image Analysis, Sediments and Paleoenvironments*, P. Francus, Ed. (Kluwer, Dordrecht, Netherlands, in press).
11. D. N. Schmidt, S. Renaud, J. Bollmann, R. Schiebel, H. R. Thierstein, *Mar. Micropaelontol.*, in press.

Downloaded from www.sciencemag.org on January 2, 2007

12. D. N. Schmidt, H. R. Thierstein, J. Bollmann, in preparation.
13. G. Chapelle, L. S. Peck, *Nature* **399**, 114 (1999).
14. Materials and methods are available as supporting material on *Science* Online.
15. S. M. Stanley, *Evolution* **27**, 1 (1973).
16. S. J. Gould, *J. Paleontol.* **62**, 319 (1988).
17. R. Cifelli, *Syst. Zool.* **18**, 154 (1969).
18. R. D. Norris, *Paleobiology* **17**, 388 (1991).
19. H. P. Luterbacher, I. Premoli-Silva, *Rev. Ital. Paleontol. Stratigr.* **70**, 67 (1964).
20. A. D. Hecht, *J. Foram. Res.* **6**, 295 (1976).
21. S. Mulitza, A. Dürkoop, W. Hale, G. Wefer, H. S. Niebler, *Geology* **25**, 335 (1997).
22. G. Wefer, W. H. Berger, J. Bijma, G. Fischer, in *Use of Proxies in Paleoceanography*, G. Fischer, G. Wefer, Eds. (Springer, Berlin, 1999), pp. 1–68.
23. J. C. Zachos, M. Pagani, L. Sloan, E. Thomas, K. Billups, *Science* **292**, 686 (2001).
24. J. H. Lipps, *Evolution* **24**, 1 (1970).
25. P. N. Pearson *et al.*, *Nature* **413**, 481 (2001).
26. E. Vincent, W. H. Berger, in *The Sea*, C. Emiliani, Ed. (Wiley, New York, 1981), vol. 7, pp. 1035–1119.
27. K.-Y. Wei, J. P. Kennett, *Paleoceanography* **1**, 67 (1986).
28. P. N. Pearson, M. R. Palmer, *Nature* **406**, 695 (2000).
29. K. G. MacLeod, B. T. Huber, T. Pletsch, U. Röhl, M. Kucera, *Paleoceanography* **16**, 133 (2001).
30. S. L. D'Hondt, M. A. Arthur, *Paleoceanography* **10**, 123 (1995).
31. M. Knappertsbusch, A. Mackensen, and R. Norris generously provided foraminiferal samples, originally taken by DSDP/ODP. We thank W. Berggren, A. Halliday, C. Hemleben, S. d'Hondt, E. Jansen, D. Kroon, M. Kucera, J. McKenzie, R. Norris, N. Shackleton, E. Thomas, and D. Vance for discussion and support. Funding was provided by the Swiss National Science Foundation.

Supporting Online Material
www.sciencemag.org/cgi/content/full/303/5655/207/DC1
Materials and Methods
SOM Text
Tables S1 to S5

19 August 2003; accepted 1 December 2003

Widespread Intense Turbulent Mixing in the Southern Ocean

Alberto C. Naveira Garabato,[1]* Kurt L. Polzin,[2] Brian A. King,[3] Karen J. Heywood,[1] Martin Visbeck[4]

Observations of internal wave velocity fluctuations show that enhanced turbulent mixing over rough topography in the Southern Ocean is remarkably intense and widespread. Mixing rates exceeding background values by a factor of 10 to 1000 are common above complex bathymetry over a distance of 2000 to 3000 kilometers at depths greater than 500 to 1000 meters. This suggests that turbulent mixing in the Southern Ocean may contribute crucially to driving the upward transport of water closing the ocean's meridional overturning circulation, and thus needs to be represented in numerical simulations of the global ocean circulation and the spreading of biogeochemical tracers.

The meridional overturning circulation (MOC) results primarily from downwelling at a few selected regions in the North Atlantic and the Southern Ocean and from upwelling elsewhere in the ocean (*1*, *2*). Precisely where and at what rate this upwelling occurs, and what physical processes drive it, are poorly known variables that seriously limit the physical relevance of ocean circulation models under present and changed climate conditions (*2*). If the MOC is primarily closed by diapycnal turbulent mixing, an advective/diffusive model (*1*) implies a globally averaged diapycnal diffusivity K_ρ of 10^{-4} m^2 s^{-1} below ~1000 m. In contrast, observations of turbulence (*3*) and dye diffusion (*4*) in the open ocean pycnocline (above ~1000 m) have revealed background diffusivities that are an order of magnitude smaller. This motivated proposals that upwelling may be primarily effected by mesoscale eddies acting on the southward-shoaling isopycnals of the Southern Ocean (*5*–*7*). In recent years, however, large ($K_\rho \geq 10^{-4}$ m^2 s^{-1}) diapycnal diffusivities have been shown to occur over rough topography (*8*, *9*). But an assessment of whether topographically enhanced mixing can account for a globally averaged diffusivity of 10^{-4} m^2 s^{-1} at any depth is prevented by the difficulty of direct measurements of diapycnal mixing, with vast regions of the ocean (notably, the Southern Ocean) remaining essentially unsampled.

We used a novel technique (*10*) to begin filling the void of diapycnal mixing observations in the Southern Ocean. The technique enables us to estimate profiles of K_ρ from observed profiles of temperature, salinity, pressure, and current velocity (*11*). It relies on the premise that turbulent mixing at scales of a centimeter or less can be related to the more easily measured intensity of internal waves, whose nonlinear interaction initiates an energy cascade to smaller scales that results in turbulent mixing (*12*, *13*). Internal wave intensity is quantified in terms of vertical gradients of density and horizontal velocity on a scale of tens to hundreds of meters. Our study focuses on the southeast Pacific/southwest Atlantic sector of the Southern Ocean, where a total of 346 profiles of the required variables were obtained during five different cruises between 1993 and 1999 (colored diamonds in Fig. 1).

The study region hosts a wide range of bathymetric and oceanographic conditions. Bottom topography is characterized by a series of nearly featureless, well-sedimented abyssal plains in the southeast Pacific and is much more complex in the southwest Atlantic (Fig. 1). There, the geologically recent separation of the South American and Antarctic plates has given

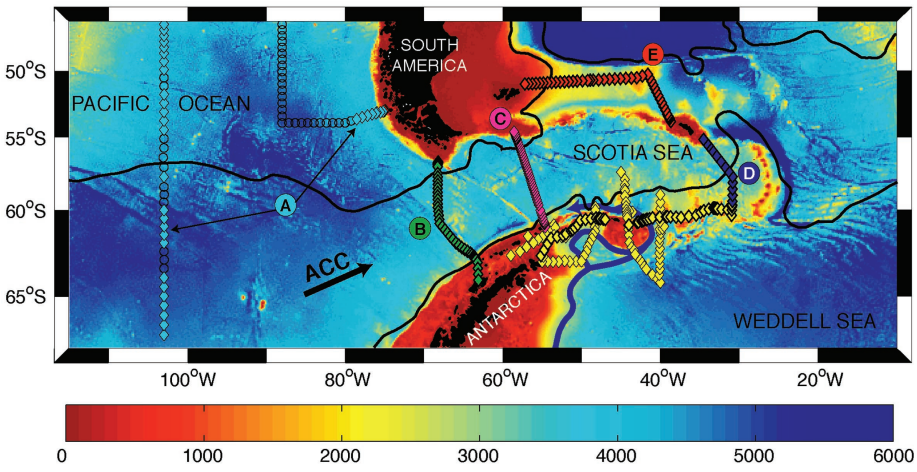


Fig. 1. Bathymetry (*43*) of the study region. CTD/LADCP stations used in this study are shown by colored diamonds. Bold diamonds mark the section plotted in Fig. 2, with colors and circled letters denoting the stations used in constructing the panels in Fig. 3 (stations indicated by yellow diamonds were not used in Fig. 3). Open circles mark stations where only CTD data are available (these were used in strain calculations). The black lines indicate the northern and southern boundaries (*44*) of the ACC, whose direction of flow is indicated by the black arrow. The thick blue arrow marks the path of the deep boundary current transporting Antarctic Bottom Water from the Weddell Sea into the Scotia Sea (*25*).

[1]School of Environmental Sciences, University of East Anglia, Norwich NR4 7TJ, UK. [2]Woods Hole Oceanographic Institution, Woods Hole, MA 02543, USA. [3]Southampton Oceanography Centre, Southampton SO14 3ZH, UK. [4]Lamont-Doherty Earth Observatory, Palisades, NY 10964–8000, USA.

*To whom correspondence should be addressed. E-mail: a.naveira-garabato@uea.ac.uk

Downloaded from www.sciencemag.org on January 2, 2007